ANNALS OF GEOPHYSICS, 59, 6, 2016, G0652; doi:10.4401/ag-6765

Geomagnetic coast effect at two Croatian repeat stations

Eugen Vujić*, Mario Brkić

University of Zagreb, Faculty of Geodesy, Zagreb, Croatia

Article history
Received March 11, 2015; accepted November 22, 2016.
Subject classification:
Geomagnetic repeat station, Geomagnetic transfer function, Inductive arrows, Geomagnetic coast effect.

ABSTRACT

Knowledge of inductive effects is important for the reliability of geomagnetic surveys as well as reduction of measurements, and hence for the accuracy of models and maps of the Earth's magnetic field. Detection of anomalous induced fields, due to the geomagnetic coast effect, was carried out by the transfer function method to estimate the induction arrows indicating areas of anomalous induced currents. To determine the transfer function at the two coastal Croatian repeat stations used in this study, the so-called geomagnetic plane-wave events from July 2010 were used. Analysis of transfer functions for Krbavsko polje and Sinjsko polje first order repeat stations, using observatories Grocka and Tihany as references, revealed the existence of the Adriatic coastal effect on periods of 10-65 minutes.

1. Introduction

Following the establishment of the Croatian Geomagnetic Repeat Station Network, a series of geomagnetic surveys has been performed from 2004 to 2010, with the aim of obtaining reliable geomagnetic data over Croatia [Brkić et al. 2013]. The reliability of such data, as well as derived products and models such as maps relies, among other factors, on the consistency between observations made at geomagnetic stations on one hand, and those made at reference observatories on the other hand. A local cause of inconsistencies is given by electromagnetic effects caused by different electric conductivity values of the lithosphere below stations and observatories. Such differences can be explored with simultaneous measurements of geomagnetic field variations in the context of deep geomagnetic sounding [Banks 1973, Armadillo et al. 2001]. Geomagnetic sounding methods are used to model subsurface electrical conductivity and, on a regional scale, they allow to determine lateral conductivity contrasts in the Earth's crust and upper mantle. Such contrasts produce anomalous induced magnetic fields, which need to be separated from the sum of the primary external magnetic fields produced in the Earth's magnetosphere and ionosphere and of those they induce in the Earth's interior (secondary) [Banks 1973, Gough et al. 1973, Hitchman et al. 2000].

An example of such anomalous induced fields, are those arising in proximity of coasts because of the contrast of electrical conductivity at the interface continent-ocean. In this case, time variations of the vertical component of the Earth's magnetic field have enlarged amplitudes, and correlate positively with the horizontal component at the close overland positions [Parkinson and Jones 1979]. This phenomenon is called "geomagnetic coast effect". In some cases, there are coastal regions where tectonic anomalies are spatially large and this effect is absent [Parkinson and Jones 1979, and references therein]. This effect is very intense during geomagnetic storms and substorms, but can occur also under quiet geomagnetic conditions. Its maximum intensity is achieved on periods between 30 and 90 minutes, and its influence can be measured on distances larger than 150 km inland from a coast [Parkinson and Jones 1979, Viljanen et al. 1995, Srivastava et al. 2001]. The models that explain the coastal effect are based on the electromagnetic induction (by the time-varying ionospheric and magnetospheric magnetic fields) contrasts: in the crust and upper mantle under continents and oceans (due to their prominently different electrical conductivities), and/or in the oceans and continents (ocean water has much higher electrical conductivity with respect to the land masses). An electromagnetic induction in the oceans could be also due to their motion across the Earth's magnetic field originating in the core and in the lithosphere [Parkinson and Jones 1979].

As part of a bilateral project "Joint Croatian-Hungarian Geomagnetic Survey and Model" (2009-2012) a number of absolute measurements and a dataset consisting of measurements of dIdD variometer (with Overhauser effect proton sensor) were gathered at

three Croatian repeat stations. Csontos et al. [2012] indicated the possible existence of geomagnetic effect of the coast in front of the Adriatic Sea, and this result was the reason for further investigation of inductive effects at the coastal Croatian repeat stations, here described and discussed.

2. Transfer function method and data

The transfer function method for detection and separation of anomalous induced fields due to conductivity contrasts from the normal induced and primary external fields, derives widely from the work of Parkinson [1959] and Wiese [1962]. In this context, let the so-called normal magnetic field $\mathbf{B}_n=(X_n, Y_n, Z_n)$ be defined as the vector sum of the primary external field (produced by electric currents flowing in the ionosphere and magnetosphere) and of the secondary internal magnetic field caused by currents in a laterally homogeneous, vertically stratified Earth's interior, which are induced by the external magnetic field variations. The local field $\mathbf{B} = (X, Y, Z)$ at any point on the Earth surface is then given by the vector sum of $\mathbf{B}_n$ and a local anomaly field $\mathbf{B}_{ia}=(X_{ia}, Y_{ia}, Z_{ia})$ caused by induced currents related to local anomalies/conductivity contrasts of the underground electric conductivity. In the case of the vertically stratified Earth's interior, the transfer function approach assumes that a linear relationship exists between $\mathbf{B}_{ia}$ and $\mathbf{B}_n$ in the frequency domain, i.e. between the Fourier transforms of $\mathbf{B}_{ia}$ and $\mathbf{B}_n$ [Banks 1973]. It is assumed that the local field $\mathbf{B}_{ia}$ is induced by the spatially homogenous field $\mathbf{B}_n$, and due to linearity of the Maxwell's equations, there has to be a linear relationship between inducing ($\mathbf{B}_n$) and induced ($\mathbf{B}_{ia}$) fields [Schmucker 1970, Lilley and Bennett 1973]. This relationship can be written in matrix form as [Banks 1973]:

$$\begin{pmatrix} X^*_{ia} \\ Y^*_{ia} \\ Z^*_{ia} \end{pmatrix} = \begin{pmatrix} W_{XX} & W_{XY} & W_{XZ} \\ W_{YX} & W_{YY} & W_{YZ} \\ W_{ZX} & W_{ZY} & W_{ZZ} \end{pmatrix} \cdot \begin{pmatrix} X^*_n \\ Y^*_n \\ Z^*_n \end{pmatrix} \qquad (1)$$

where the coefficients W_{XX}, W_{XY}, ..., W_{ZZ} of the matrix $\mathbf{W}$ denote the frequency-dependent transfer function between $\mathbf{B}_n$ and $\mathbf{B}_{ia}$, and the asterisk * denotes the complex Fourier transform. Now the problem given by the above equations can be reduced onto estimation of the components of the normal external field at each measurement point. The transfer function can be obtained from Equation (1) after some simplifying assumptions, based on the generally valid observation that the magnitude of Z^*_n is small compared to Z^* at mid latitudes, which is generally satisfied in the case of the vertically stratified interior and when the primary external field has relatively large wavelengths [Banks 1973, and references therein, Viljanen et al. 1995]. This means that the products of Z^*_n with W_{XZ}, W_{YZ} and W_{ZZ} can be neglected. Further, it is assumed that X^*_n and Y^*_n are independent of Z^*_n, and that they can be replaced by X^* and Y^*, respectively [Banks 1973]. In this case, Equation (1) reduces to [Banks 1973, Viljanen et al. 1995, Hitchman et al. 2000, Srivastava et al. 2001]:

$$Z^*_{ia} = AX^* + BY^* + \varepsilon \qquad (2)$$

where Z^*_{ia} is the difference between Z^* measurements at an anomalous (coastal) point and at a reference geomagnetic observatory, A and B are coefficients of the simplified transfer function, and ε is the residual of Z^*_{ia} that is not correlated to X^* and Y^*, i.e. instrumental noise and the neglected correlation with Z^*_n. All the quantities from Equation (2) can be obtained from the time series at the anomalous (coastal) point and at the normal (reference) point, as explained in the following. Also, the transfer functions given by the other two equations in (1), i.e. those for X^*_{ia} and Y^*_{ia}, can not be determined from a single station analysis of this kind [Schmucker 1970, Banks 1973, Lilley and Bennett 1973].

A normal point is regarded to be the location where a variometer measures variations of the Earth's magnetic field, without influence of anomalous induced electric currents. Generally a geomagnetic observatory satisfies this requirement. Magnetic fields produced by induced currents below normal points will be independent of the direction of the time varying external field, so that no persistent correlations exists between Z^*_{ia} and the horizontal field (i.e., $A=B=0$ in Equation (2)). It is assumed that under the geomagnetic observatories is a conductivity structure characterised by a lateral homogeneity and vertical stratification. On the other hand, a variometer station located close to a conductivity anomaly will measure vector sum of the normal field $\mathbf{B}_n$ and an anomaly field $\mathbf{B}_{ia}$ induced by the horizontal components of $\mathbf{B}_n$ according to Equation (2) [Banks 1973, Hitchman et al. 2000, Srivastava et al. 2001]. If lateral variations of $\mathbf{B}_n$ over the distance separating an anomalous point from the corresponding reference observatory are negligible in comparison to the induced anomaly field itself, Z^*_{ia} in Equation (2) can be identified with the difference between the vertical components of the total field measured with at the variometer station and the observatory, respectively. The complex geomagnetic transfer function can then be calculated by solving Equation (2) with respect to the coefficients A and B. Stable solutions are given by [Schmucker 1970, Banks 1973, Gough et al. 1973]:

$$A = \frac{S_{ZX}S_{YY} - S_{ZY}S_{YX}}{S_{XX}S_{YY} - |S_{YX}|^2} \tag{3a}$$

$$B = \frac{S_{ZY}S_{XX} - S_{ZX}S_{XY}}{S_{XX}S_{YY} - |S_{YX}|^2} \tag{3b}$$

where S_{XX}, S_{XY}, etc. denote the cross-spectra calculated from the horizontal components X and Y of the total field measured at the anomalous point, e.g. $S_{XX} = X\,\overline{X}^*/T_0$, $S_{XY} = X\,\overline{Y}^*/T_0$, where T_0 is the duration of the time series, and $\overline{X}^*$, $\overline{Y}^*$ denote the complex conjugates of X^* and Y^*, respectively.

The complex transfer coefficients A and B obtained in this manner define a so-called induction arrow [Banks 1973], whose real part describes the in-phase response to variations of the horizontal field, with amplitude and azimuth given by Equations (4a) and (4b), respectively:

$$Amp_r = \sqrt{[\mathrm{Re}(A)]^2 + [\mathrm{Re}(B)]^2} \tag{4a}$$

$$Az_r = \arctan\left\{\frac{\mathrm{Re}(B)}{\mathrm{Re}(A)}\right\}. \tag{4b}$$

The quadrature response is defined in an analogous manner using the imaginary components of A and B. The induction arrow rotated by 180° points towards the cause of $\mathbf{B}_{ia}$ [Banks 1973, Viljanen et al. 1995].

Magnetic storms or substorms are commonly used for finding the transfer function at a given location. To these phenomena correspond time variations of the external magnetic field that are produced by independent currents systems with acceptable levels of strength in a wide range of frequencies. Equation (2) was obtained under the above assumptions, and implies homogeneity of time variation of the horizontal external field, over areas where normal and possibly anomalous magnetic fields are monitored by variometers [Banks 1973, Viljanen et al. 1995, Srivastava et al. 2001].

In addition to the abovementioned intervals of increased geomagnetic activity, it is possible to use so-called plane wave events [Viljanen et al. 1995]. Such events are associated with laterally homogeneous electromagnetic plane waves traveling in the underground, in which case a vertical $\mathbf{B}_{ia}$ is generated where the wave crosses regions with lateral electrical conductivity heterogeneities. Necessary condition for using planar wave events is the existence of a good linear correlation between the horizontal field components at the reference point and at the point where the transfer function is calculated. Furthermore, the parameter R given by Equation (5), expressing the relative difference between field variations at the variometer site and the reference station [Viljanen et al. 1995], should be relatively small (possibly below 25%):

$$R(E) = 100 \cdot \frac{\sigma(E - E_{ref})}{\max(|E_{ref}|)} \tag{5}$$

where R is expressed in percent, E is the time variation

GCK		THY		Time interval (UTC)
$R(X)$/%	$R(Y)$/%	$R(X)$/%	$R(Y)$/%	
		KRBP		
3.9	13.2	9.3	9.6	15:31-17:39
4.0	12.6	8.2	10.0	15:39-17:47
4.7	11.4	6.9	10.4	15:55-18:03
6.2	11.7	7.8	8.4	16:10-18:18
5.1	8.4	9.9	6.2	16:31-18:39
3.2	5.6	9.1	5.7	16:51-18:59
3.1	23.5	11.8	11.2	14:07-16:15
		SINP		
14.7	17.9	20.5	22.6	08:09-10:17
9.9	16.9	19.2	25.3	08:34-10:42
10.8	14.2	18.5	23.0	08:37-10:45
11.0	11.9	18.2	19.1	08:39-10:47
7.3	16.0	10.8	11.4	17:27-19:35
6.6	9.4	9.4	8.9	17:42-19:50
6.2	9.7	9.0	8.3	17:46-19:54

Table 1. Parameters $R(X)$ and $R(Y)$ between the observatories GCK and THY and repeat stations KRBP and SINP, and selected time intervals of plane wave events on July 21 and 22, 2010, for KRBP, and July 26, 2010, for SINP.

(with respect to the quiet-night value) of geomagnetic components X or Y at the point for which the transfer function is calculated, the subscript *ref* refers to the reference point, and σ is the standard deviation.

The possible existence of inductive effects in Croatian repeat stations was postulated already after the 2010 survey. At that time, the survey at Krbavsko polje (KRBP) and Sinjsko polje (SINP) was performed according to the IAGA standards [Newitt et al. 1996] and MagNetE recommendations (http://www-app3.gfz-potsdam.de) using the Hungarian nonmagnetic theodolite Zeiss Theo 020A with fluxgate sensor and DMI D&I electronic unit, and GemSyS GMS-19G Overhauser effect Proton Precession Magnetometer, as well as Overhauser effect dIdD variometer. In that occasion, it was noticed that the spatial gradient of total field intensity was correlated with the spatial gradient of the eastern component of the field (Y), whereby the phenomenon was more strongly expressed near the coast, leading to the hypothesis that it was caused by the conductivity contrast between Adriatic Sea and mainland [Csontos et al. 2012].

Because only one substorm occurred during the whole 2010 survey [Gjerloev 2012], plane wave events were instead used to calculate the transfer functions at KRBP and SINP. Suitable events (Table 1) have been selected from geomagnetic time series of a repeat station and the corresponding reference observatory, using a sliding window in the time domain to search for 128-minutes-long intervals that satisfy the abovementioned plane wave conditions. Two observatories, Grocka (GCK) in Serbia and Tihany (THY) in Hungary, have been used as reference points for the calculation of the induction arrows at SINP and KRBP (Figure 1). The main objective was to confirm whether there is a geomagnetic effect of the Adriatic coast at the considered repeat stations, whose distances from the Adriatic Sea coast are of about 53 km (KRBP) and 22 km (SINP).

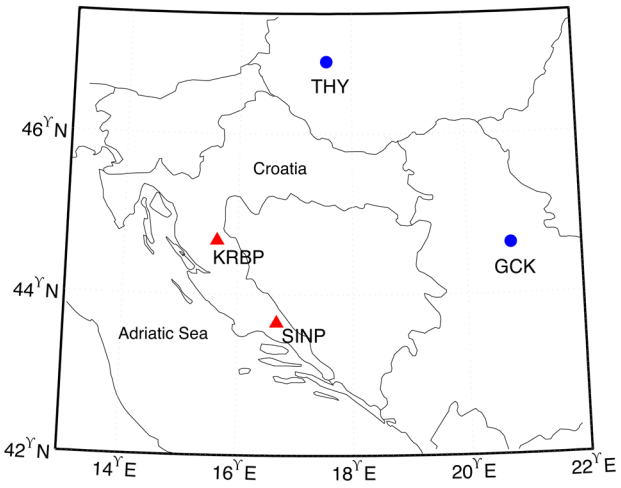

Figure 1. The positions of two Croatian repeat stations KRBP and SINP, together with two reference observatories (GCK and THY). In detail, latitude, longitude and elevation of KRBP are 44.7° N, 15.6° E, 648 m, for SINP geographical coordinates are 43.6° N, 16.7° E, 296 m.

3. Results and discussion

Using plane wave events from Table 1 and the Equations (3)-(4), the simplified transfer functions between the horizontal and vertical Fourier components were calculated for periods comprised between 2 and 128 minutes, considering GCK and THY as references (Table 2). The cross-spectra of geomagnetic components have been calculated using the fast Fourier transform (FFT) of the time series corresponding to the plane wave events listed in Table 1. In the time domain the adjustable Tukey window (tapered cosine window) was applied. Multiplication of the signal with a suitable window in the time domain previous to the FFT is necessary to avoid high-frequency artifacts. Windows are smoothing functions that peak in the middle frequencies and decrease to zero at the edges, thus reducing the effects of the discontinuities as a result of finite duration [Bendat and Piersol 2000]. Further, each cross-spectra used in Equation (3) must be a mean value from a number of variation events [Schmucker 1970, Gough et al. 1973], and in this case they were averaged over the events given in Table 1 for KRBP and SINP, respectively.

Seven plane wave events each of 128 min duration were selected (Table 1). The periods used for induction arrow calculations have been chosen to be evenly distributed, on a logarithmic scale, between the sampling interval of 1 minute and the total event duration of 128

Station	Amp_r	$Az_r/°$	$\sigma_{15\text{-}60}$	Amp_i	$Az_i/°$	Amp_r	$Az_r/°$	$\sigma_{15\text{-}60}$	Amp_i	$Az_i/°$
			GCK					THY		
KRBP	0.30 ±0.07	266 ±17	±0.08	0.12 ±0.08	176 ±113	0.35 ±0.07	259 ±10	±0.07	0.11 ±0.06	197 ±92
SINP	0.37 ±0.09	233 ±8	±0.05	0.08 ±0.06	123 ±98	0.34 ±0.14	234 ±8	±0.13	0.12 ±0.07	142 ±125

Table 2. Results of the transfer functions analysis for KRBP and SINP, using observatories GCK and THY as a reference point. All entries are written as *mean*±*standard deviation*. *Amp* and *Az* are the lengths and azimuths of induction arrows, indices (*r*) and (*i*) apply to the real and imaginary arrows, and $\sigma_{15\text{-}60}$ is the standard deviation of the length of the real arrows in the period interval of 15-60 min. The values refer to the average and the standard deviation of data obtained from periods of (10.7 min, 12.8 min, 18.3 min, 25.6 min, 32.0 min and 64.0 min) for KRBP, and of (12.8 min, 18.3 min, 21.3 min, 42.7 min and 64.0 min) for SINP.

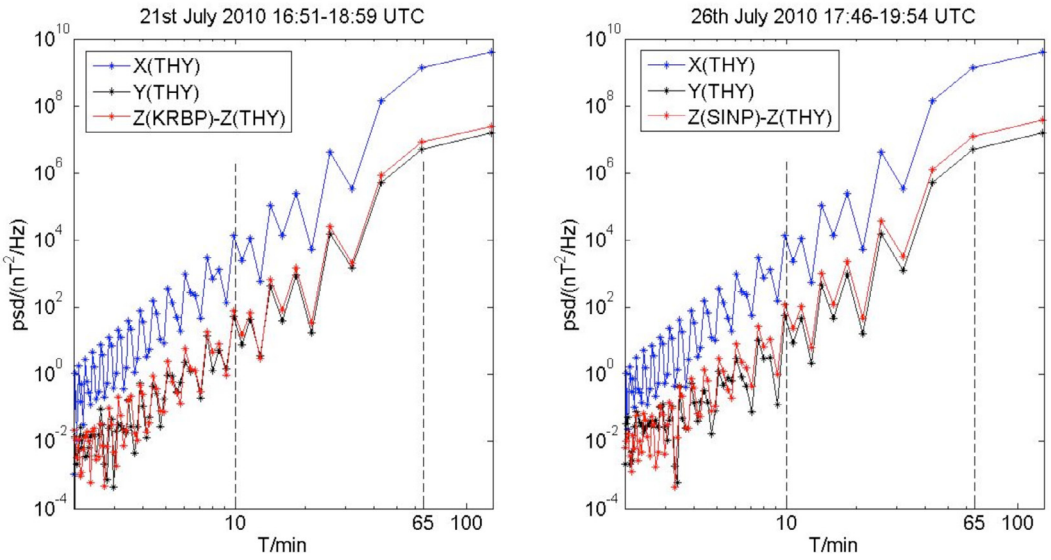

Figure 2. Left: Power spectrum density (*psd*) as a function of period (*T*), of *X* and *Y* components from THY, and of the difference of *Z* component at KRBP and THY, for time interval on July 21, 2010, 16:51-18:59 UTC. Right: the same as for KRBP, but for another selected time interval at SINP (July 26, 2010, 17:46-19:54 UTC).

minutes. Figure 2 shows the power spectrum of *X*, *Y* and *Z* components of the two selected plane wave events, as an example. The powers of components generally increase with period, and have the highest values for *X* component. *R* values calculated with Equation (5) were <12% for *X* and <24% for *Y* in KRBP, and <21% and <26% for *X* and *Y* in SINP. Furthermore, correlation coefficients between the horizontal field components measured with the variometer and at the reference observatory were >0.97 for KRBP and >0.93 for SINP. These results confirm the validity of the plane wave assumption and thus the suitability of the chosen time series intervals for the calculation of induction arrows.

The real (i.e. in-phase) induction arrows are characterized by relatively small amplitudes (<0.4, see Table 2) and point consistently to the West at KRBP and to the South West at SINP over the whole frequency range. The imaginary (quadrature) induction arrows, on the other hand, are smaller in amplitude (<40% of the real arrows) and are characterized by much more scattered directions, depending on the chosen period. These directions are, on average, almost opposite to those of the real induction arrows. The angular scatter of the real induction arrows is in the range of 8-17°, while the scatter of the imaginary arrows is much higher, i.e. in the range of 92-125°. Further, the lower dispersion of real induction arrows azimuths at SINP is observed, compared to KRBP when using different reference points. The scatter of the real induction arrows is random for both stations, i.e. it does not show a systematic correlation with the corresponding period. It appears that the real induction arrows scatter at KRBP is much smaller if referred to THY instead of GCK, and one could presume that THY is a more representative reference station for KRBP. A similar reasoning does not hold for SINP, where the scatter is the same for both reference stations.

The general observation is that $\mathbf{B}_n$ is reconstructed from data collected at a different place while being attributed to the same location as far as the equations are concerned. Deviations of the results for amplitudes and azimuths of induction arrows at the same periods, when GCK and THY are used separately at any point, could be caused by the fact that the selected events do not fully correspond to laterally homogeneous plane wave model. It should not be forgotten that the field generated in the ionosphere and magnetosphere can have some degree of heterogeneity over the distances between variometers and reference stations, which are in this case much larger than the thickness of the ionosphere. Moreover, a presence of anomalous field in horizontal components of the inducing field is possible [Armadillo et al. 2001], so the reference observatories could also not be the ideal normal points. Finally, the mentioned deviations can be attributed also to the effect of spatial electric conductivity gradients on the mainland.

At KRBP repeat station inductive coast effects were found at six periods, and at SINP at five periods (Table 2). Figures 3a and 3b show the corresponding real and imaginary induction arrows for both repeat stations, respectively, with respect to the reference observatories. A relatively small value of the standard deviation of the amplitudes of the real induction arrows, for periods of 15-60 min (Table 2), can be one of the indicators of the geomagnetic coast effect [Parkinson and Jones 1979]. Additional indicators of this effect can be: amplitude of the imaginary induction arrows should, at the same pe-

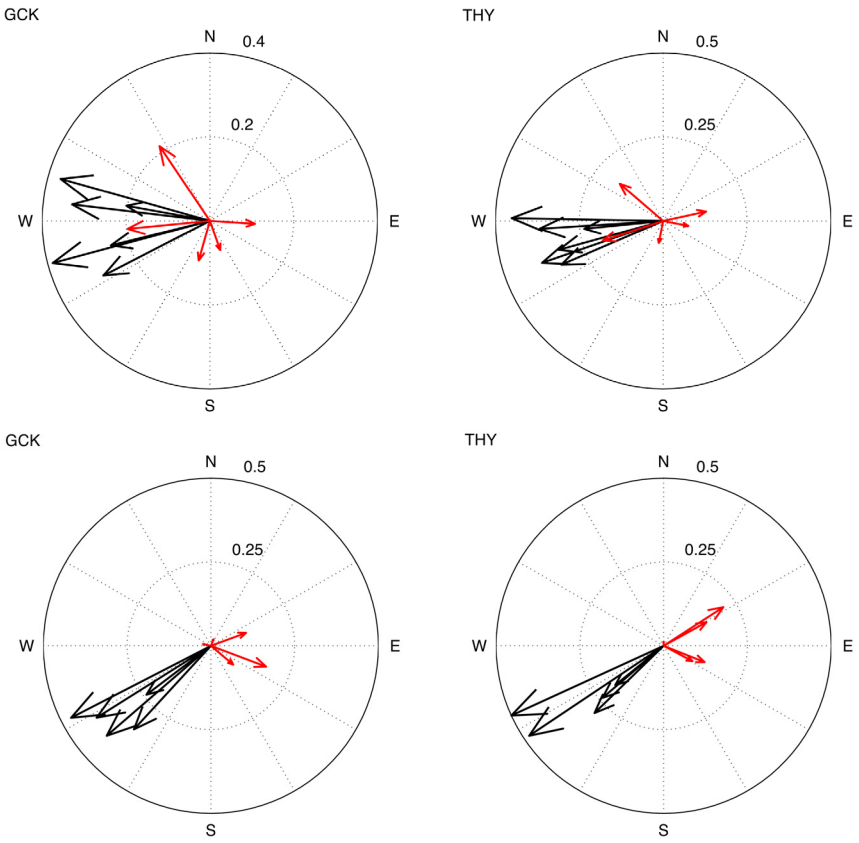

Figure 3. (a) Real (black) and imaginary (red) induction arrows for KRBP, with GCK and THY as reference points. These arrows have been obtained for periods of 10.7 min, 12.8 min, 18.3 min, 25.6 min, 32.0 min and 64.0 min. (b) Real (black) and imaginary (red) induction arrows for SINP, with GCK and THY as reference points. These arrows have been obtained for periods of 12.8 min, 18.3 min, 21.3 min, 42.7 min and 64.0 min.

riods, be 0.25-0.5 times lower than that of the real ones; in addition, the imaginary arrows have a greater range of azimuths, i.e. they are more random and are more susceptible to the period. Figure 4 illustrates an example of real induction arrows at the period T = 18.3 min for KRBP (amplitude of 0.24) and SINP (amplitude of 0.50), with respect to a reference point THY. At the repeat stations the real induction arrows are directed toward the coast of the Adriatic Sea.

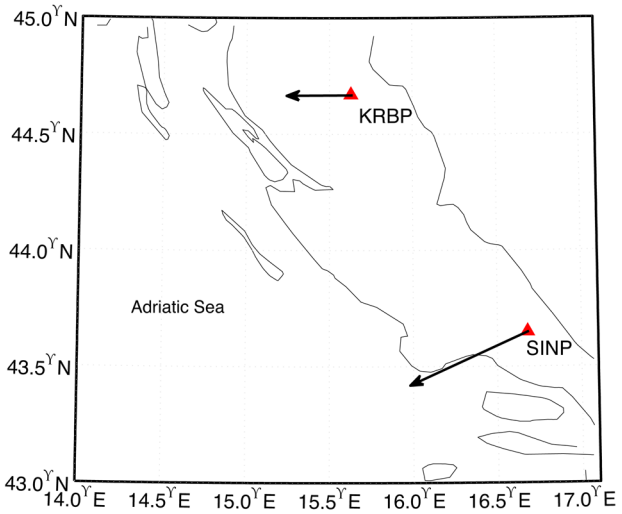

Figure 4. Real induction arrows at period $T = 18.3$ min for KRBP (amplitude of 0.24) and SINP (amplitude of 0.50), with respect to the reference point THY.

4. Conclusion

Coastal inductive effects at the Krbavsko polje and Sinjsko polje repeat stations have been investigated with the geomagnetic transfer function method during plane wave events, using Grocka and Tihany observatories as reference. The real induction arrows at the repeat stations point towards the Adriatic Sea, where the anomalous induced currents are more intense. The geomagnetic coastal effects were found in both repeat stations and for periods from 10.7 min to 64 min. This work confirmed geomagnetic coastal effects near the eastern coast of Adriatic for the first time; the effects found near the western Adriatic coast were described in Armadillo et al. [2001].

A practical consequence is that data reduction at the stations near the eastern coast of Adriatic has to be performed with proper caution. It is advisable to use the recordings from on-site triaxial variometer for data reduction, i.e. to choose the appropriate time intervals as free as possible from the anomalous induced effects. It is also recommended to apply the other methods in order to investigate inductive effects at sites of the Basic Geomagnetic Network of the Republic of Croatia. The

method for the transfer functions estimation in frequency-domain used in this work is based on a standard least squares procedure [Schmucker 1970]. The methods based on a robust estimation of the transfer functions in frequency-domain can also be used, see e.g. Hitchman et al. [2000] and references therein. Additionally, the estimations of induction arrows can be performed in the time-domain; an example is given in Viljanen et al. [1995] and references therein. Finally, the method used in this work cannot be applied to points beyond a certain critical distance (up to several hundreds of km at mid latitudes) from the closest reference observatory. The two reference observatories used here were selected because they were the closest to the repeat stations in different directions (closer than 410 km), and far away from the sea coast. In the future, it can be expected that the data from Croatian observatory Lonjsko polje will be used in such studies, since this observatory is closer to the near-coastal repeat stations than the other observatories, and still far away from the Adriatic Sea.

Acknowledgements. Data used in this paper are product of projects funded by the Ministry of Science, Education and Sports, State Geodetic Administration, as well as Ministry of Defence of the Republic of Croatia. The results presented in this paper rely on data collected at magnetic observatories. We thank the national institutes that support them and INTERMAGNET for promoting high standards of magnetic observatory practice. The authors are very thankful to Dr. R. Egli and anonymous reviewers for their constructive comments and suggestions that significantly improved the manuscript.

Data and sharing resources

The one-minute GCK and THY data were downloaded from Intermagnet Web site (www.intermagnet.org).

References

Armadillo, E., E. Bozzo, V. Cerv, A. De Santis, D. Di Mauro, M. Gambetta, A. Meloni, J. Pek and F. Speranza (2001). Geomagnetic depth sounding in the Northern Apennines (Italy), Earth Planets Space, *53*, 385-396.

Banks, R. (1973). Data processing and interpretation in geomagnetic deep sounding, Phys. Earth Planet. Int., *7*, 339-348.

Bendat, J.S., and A.G. Piersol (2000). Random data: Analysis and measurement procedures, John Wiley & Sons Inc., USA.

Brkić, M., E. Vujić, D. Šugar, E. Jungwirth, D. Markovinović, M. Rezo, M. Pavasović, O. Bjelotomić, M. Šljivarić, M. Varga and V. Poslončec-Petrić (2013). Basic Geomagnetic Network of Republic of Croatia 2004-2012, with the geomagnetic field maps at 2009.5 epoch, Ed.: M. Brkić, Croatian Geodetic Administration, Zagreb, ISBN: 978-953-293-521-9, (in Croatian).

Csontos, A., D. Šugar, M. Brkić, P. Kovács and L. Hegymegi (2012). How to control a temporary DIDD based observatory in the field?, Annals of Geophysics, *55* (6), 1085-1094.

Gough, D.I., J.H. de Beer and J.S.V. van Zijl (1973). A Magnetometer Array Study in Southern Africa, Geophys. J. R. Astr. Soc., *34*, 421-433.

Gjerloev, J.W. (2012). The SuperMAG data processing technique, J. Geophys. Res., 117, A09213, doi:10.1029/2012JA017683.

Hitchman, A.P., F.E.M. Lilley and P.R. Milligan (2000). Induction arrows from offshore floating magnetometers using land reference data, Geophys. J. Int., 140, 442-452.

Lilley, F.E.M., and D.J. Bennett (1973). Linear relationships in geomagnetic variation studies, Phys. Earth Planet. In., 7, 9-14.

Newitt, L.R., C.E. Barton and J. Bitterly (1996). Guide For Magnetic Repeat Station Surveys, IAGA, Boulder, SAD.

Parkinson, W.D. (1959). Directions of Rapid Geomagnetic Fluctuations, Geophys. J. R. Astr. Soc., 2 (1), 1-14.

Parkinson, W.D., and F.W. Jones (1979). The Geomagnetic Coast Effect, Rev. Geophys. Space Phys., 17 (8), 1999-2015.

Schmucker, U. (1970). Anomalies of geomagnetic variations in the Southwestern United States, Bull. Scripps Inst. Oceanogr., Univ. Calif. San Diego, 13, 1-165.

Srivastava, B.J., Abbas Habiba, T. RamaGopal, D.R.K. Rao and B.M. Pathan (2001). Geomagnetic coast and other effects deduced from the new observatory at Visakhapatnam, India, Geophys. J. Int., 146, 827-832.

Viljanen, A., K. Kauristie and K. Pajunpää (1995). On induction effects at EISCAT and IMAGE magnetometer stations, Geophys. J. Int., 121, 893-906.

Wiese, H. (1962). Geomagnetische Tiefentellurik, Teil II: Die Streichrichtung der Untergrundstrukturen des elektrischen Widerstandes, erschlossen aus geomagnetischen Variationen, Geofis. Pura e Appl., 52, 83-103.

Corresponding author: Eugen Vujić,
External Associate of Faculty of Geodesy, University of Zagreb, Croatia; email: eugvujic@gmail.com.